Proceedings of the
International Conference on Mechanical Engineering 2007
(ICME2007) 29- 31 December 2007, Dhaka, Bangladesh

ICME07-FL-11

NUMERICAL INVESTIGATION OF THE TURBULENCE CHARACTERISTICS OF THE TWO-PHASE FLOW IN AN INDUSTRIAL NOZZLE

M.A. Rahman

PhD candidate, Department of Mechanical Engineering, University of Alberta, Canada.
E-mail: marahman@ualberta.ca

ABSTRACT

The main objective of this study is to get a better insight of the basic phenomena associated with air/water two-phase bubbly flows through an industrial nozzle. Two-phase bubbly flows are quite complicated transport phenomena. There are still fundamental aspects of two-phase flows; whose physical descriptions are still unknown and modeling results are questionable. Experimental observations are difficult in this case as the migration of dispersed bubbles towards the top of the pipe, due to buoyancy, causes a highly non-symmetric volume distribution in the pipe cross-section. Often existing theoretical solutions do not agree with experimental results. In the analytical analysis of mathematical formulation requires a system of non-linear differential equations. Numerical solutions using computational fluid dynamics (CFD) partially can treat two-phase flow problems. In this study, it was observed that the turbulence intensity in the air-water two-phase horizontal flow increases with air-to-liquid-ratio, ALR (2% to 4% by mass) due to increased inter-phase interactions. Another important finding is that the turbulence kinetic energy and dissipation rate is higher near the wall region of the conduit.

Keywords: CFD modeling, Two-phase flow, Air to liquid ratio, Turbulent kinetic energy and dissipation, Reynolds stresses.

1. INTRODUCTION

Due to the complex nature of the two-phase flow phenomena, a single-flow theory has not yet reached a mature stage [1]. Instead, the CFD codes enable the solution of complex flow-fields like this. However, till to date much efforts have been devoted to one-dimensional flows. Three-dimensional closed-form computational solutions and expressions for bubbly flows would provide a better insight into the basic phenomena associated with the two-phase bubbly flows.

Turbulent gas-liquid flow occurs in many engineering two-phase fields [2]. Yang et al. [2] experimentally measured turbulent fluctuations, u_f, v_f, w_f, in axial, radial and circumferential directions, respectively, and Reynolds stresses $-uv$ and $-uw$. They found that in the lower portion of the tube the turbulence fluctuations resemble to those of single-phase flow.

However, in the upper portion of the pipe, where the bubble population is high, the turbulence fluctuations are enhanced. Conversely several researches found that bubble reduces the local turbulence when compared with single-phase flow turbulence [3], [4]. It was also observed that turbulent shear stress profile is altered by the presence of bubbles promoting frictional drag reduction in the bubbly two-phase flow [5].

The transient behavior of the two-phase flow including the drag, lift and virtual mass forces that is observed in experiments captured by Deen et al. [6] successfully by the Euler-Euler approach. The Euler-Lagrange approach was used by Delnoij et al. [7] and Sokolichin et al. [8]. Sokolichin et al. [8] indicated that the Euler-Euler approach gives similar results as the Euler-Lagrange approach. The advantage of the Euler-Euler approach is that the computational demands are much lower compared to the Euler-Lagrange approach, for systems with higher dispersed void fractions. Several researchers incorporated different turbulence models in their two-phase flow simulation. Most of them uses standard k-ε model. However Reynolds-Stress models (RSM) and standard k-ω models are still need to be explored in case of two-phase flow simulation.

The overall objective of this project is to optimize the operating range of the existing steam/bitumen nozzles used in the Syncrude coker. Knowledge obtained will contribute to the development of a new series of nozzles Syncrude is currently bringing to market. In fluid coking nozzles, the gas (steam) and liquid (bitumen) mix well in upstream of the pipe prior to feeding the mixture through the nozzles. One of the physical problems in the operation of fluid coking nozzles is the development of

instabilities in the spray. This is caused by the two-phase flow pattern formed (slug/wavy annular flow) inside or upstream of the nozzle. Recent experiments conducted by the authors show that if the air to liquid ratio by mass (ALR) increases to 1.50%, the spray becomes unstable (transition occurs from bubbly flow to intermittent flow).

2. ANALYSIS AND MODELLING

The continuity equation for each phase is described as:

$$\frac{\partial}{\partial t}(\rho_k \alpha_k) + \nabla.(\rho_k \alpha_k \mathbf{u_k}) = 0 \qquad (1)$$

The momentum equation for each phase is described as:

$$\frac{\partial}{\partial t}(\rho_k \alpha_k \mathbf{u_k}) + \nabla.(\rho_k \alpha_k \mathbf{u_k u_k}) = -\alpha_k \nabla p + \rho_k \mathbf{g} + \alpha_k \mu_k \nabla^2 \mathbf{u} + \mathbf{F_{km}} \qquad (2)$$

The first term in the right hand side equation indicates the pressure force, the second term indicates the gravity force, the third term indicates viscous force and the fourth term indicates summation of all interfacial forces. The interfacial force terms can be expressed as follows:

$$\mathbf{F_{km}} = \mathbf{F_D} + \mathbf{F_L} + \mathbf{F_{TD}} + \mathbf{F_{WL}} + \mathbf{F_{VI}}M \qquad (3)$$

where, $\mathbf{F_D}$ indicates drag force, $\mathbf{F_L}$ indicates lift force, $\mathbf{F_{TD}}$ indicates turbulent dispersion force, $\mathbf{F_{WL}}$ wall lubrication force, $\mathbf{F_{VI}}M$ indicates virtual mass force. The drag force can be expressed as:

$$\mathbf{F_D} = \frac{3}{4} C_D \alpha_g \rho_l \frac{1}{d_b} \left| u_l - u_g \right| (\mathbf{u}_l - \mathbf{u}_g) \qquad (4)$$

The drag coefficient in the case of distorted bubble was proposed by Ishii and Zuber [9] as follows:

$$C_D = \frac{2}{3} Eo^{\frac{1}{2}} \qquad (5)$$

where, Eo is the dimensionless Eotvos number:

$$Eo = \frac{g \Delta \rho d_b^2}{\sigma} \qquad (6)$$

The lift force encounters the shearing motion effects in the liquid phase on the movement of the gas-phase phase, which is modeled as:

$$\mathbf{F_L} = C_L \alpha_g \rho_l (\mathbf{u}_g - \mathbf{u}_l) \times \nabla \times \mathbf{u}_l \qquad (7)$$

C_L is the lift model constant. Turbulent dispersion forces result in additional dispersion of phases from high volume fraction regions to low volume fraction regions due to turbulent fluctuations [10]. This can be expresses as:

$$\mathbf{F_{TD}} = -C_{TD} \rho_l \mathbf{n_w} \nabla \alpha_l \qquad (8)$$

Unfortunately there does not exist a universally valid value of the non-dimensional turbulent dispersion coefficient (C_{TD}) Value of 0.1 has been used successfully for bubbly flow with bubble diameters of order a few millimeters [11].

Wall lubrication force tends to push the dispersed phase away from walls. In situations where the lift force pushes bubbles towards the wall, the lubrication force acts in the opposite direction to ensure that bubbles accumulate a short distance away from the wall. This is expressed as:

$$\mathbf{F_{WL}} = -\alpha_g \rho_l \frac{\left[\mathbf{u_r} - (\mathbf{u_r}.n_w) n_w\right]}{d_b} \max\left[C_1 + C_2 \frac{d_b}{y_w}, 0\right] \qquad (9)$$

Here, u_r is the relative velocity between phases, d_b is the disperse phase mean diameter, y_w is the distance to the nearest wall, n_w is the unit normal pointing away from the wall, and C_1 and C_2 are model constants for the wall lubrication force

Virtual mass force takes into account the acceleration of the liquid in the wake of the bubble, which is expressed as:

$$\mathbf{F_{VI}}M,\mathbf{l} = \alpha_g \rho_l C_{VM} \left[\frac{D\mathbf{u}_g}{Dt} - \frac{D\mathbf{u}_l}{Dt}\right] \qquad (10)$$

where, C_{VM} a model constant with value of 0.5. the $\frac{D}{Dt}$ operators indicates the substantial derivative of the two phase. The virtual mass force is only important in cases where the particle density is less than or equal to the fluid density.

A commercial CFD package was used to solve the equations of continuity and momentum for the two-fluid mixture. The pressure-velocity coupling is obtained using the SIMPLE algorithm. A fully implicit backward difference scheme was used for the time integration. Inhomogeneous Eulerian–Eulerian two-phase model was used in the simulation. The RMS residual target of 1×10^{-4} was implemented. The boundary conditions applied in the model is described as follows:

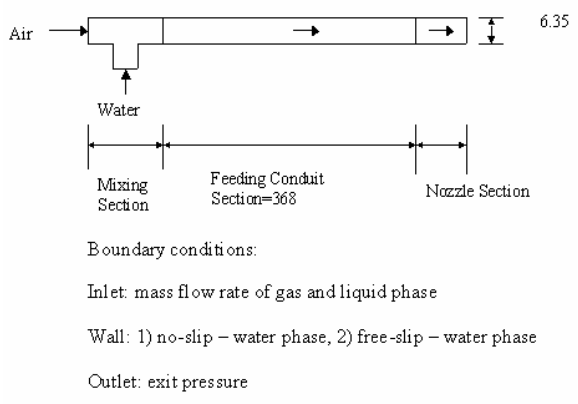

Fig 1: Experimental set-up of an industrial nozzle assembly.

All the dimensions are in millimeter. Internal diameter and length of the existing pipe is 6.35 mm and 638 mm respectively. The nozzle exit diameter would be 3.10 mm

3. RESULTS AND DISCUSSION

In Figure 2 variation of the normalized turbulent kinetic energy and large eddy dissipation in the radial direction with changing ALR is depicted. One of the important observations is that if the ALR (% by mass) increases from 2% to 4% both the turbulent kinetic energy and dissipation increases. This enhancement is significant near the wall region of the conduit. Near wall turbulent intensity is higher than in the center of the conduit. In addition, turbulence kinetic energy is higher than the dissipation in the radial direction. Thus, viscous and pressure dissipation and mean flow energy flux also involved in the turbulent energy budget. If ALR increases, turbulent intensity increases significantly due to enhanced shearing forces between the two phases.

In Figure 3, the Reynolds stresses in the radial direction for 1% ALR is depicted. It is observed that the normal stresses are higher than the shear stresses. In addition, stream-wise normal stresses are higher than the radial and span-wise normal stresses at 1% ALR. Shear stresses decay rapidly in the centre of the pipe compared with the normal stresses.

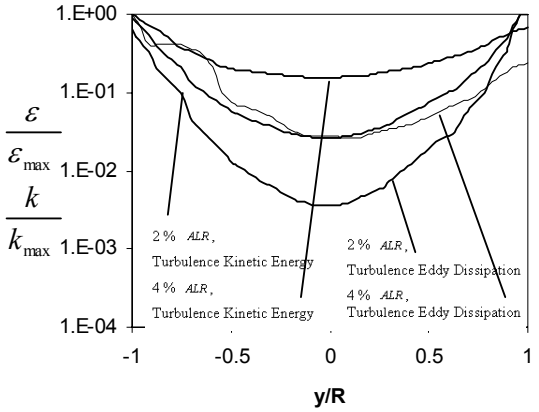

Fig 2: Normalized turbulence kinetic energy and eddy dissipation values using the $\kappa - \varepsilon$ turbulence model at 2% and 4% ALR by mass. These values are obtained 36.8 cm downstream from the inlet

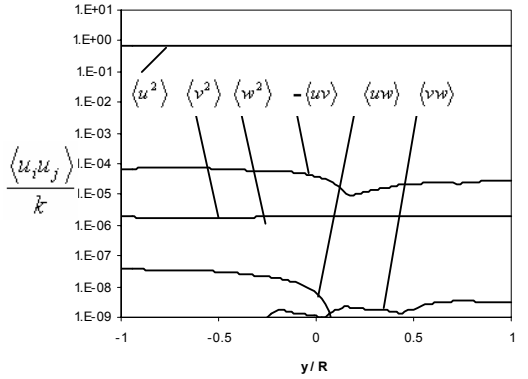

Fig 3: Reynolds stresses profile at 1% ALR by mass using the BSL Reynolds Stress model ay z=36.80 cm.

In Figure 4, the Reynolds stresses in the radial direction for 4% ALR is depicted. As expected, if the ALR is increased the principal stresses become equal to each other. On the other hand, values of the shear stresses are increased. Thus, increased ALR (4% by mass) produces more turbulent anisotropy compared to the lower ALR situation (2% by mass). This anisotropy is the result of enhanced interfacial interaction between water and air phases

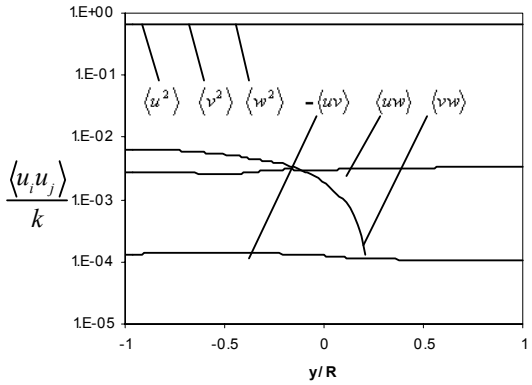

Fig 4: Reynolds stresses profile at 4% ALR by mass using the BSL Reynolds Stress model ay z=36.80 cm.

4. CONCLUSIONS

Air-water two-phase flow in an horizontal nozzle assembly was simulated numerically using the finite volume approach. Turbulence characteristics of the two-phase flow were investigated. The standard $k - \varepsilon$ and BSL Reynolds stress model was implemented as the turbulence scheme in the modeling. In this study it was observed that if the ALR (% by mass) is increased from 2% to 4%, turbulence intensity is also increased for the two-phase bubbly flow. Reynolds stresses value also increases with ALR. Normal stresses show indicial behavior at high ALR values (4%). Although at high ALR values turbulence anisotropy is increased compared to the low ALR values (2%) due to increases inter-phase interaction. In addition, turbulence kinetic energy and eddy dissipation increase with ALR values.

5. ACKNOWLEDGMENT

The authors wish to acknowledge the financial support used to carry out this study provided by Syncrude Canada Ltd, Alberta Ingenuity, and NSERC

6. REFERENCES

1. Mor, M. and Gany, A. (2004) Analysis two-phase homogenous bubbly flows including friction and mass addition. Journal of Fluids Engineering. 126(1), 102-109.
2. Yang, J., Zhang, M., Zhang, C. Su, Y., Zhu, X. (2004) Quasi 3-D measurements of turbulence structure in horizontal air–water bubbly flow. Nuclear Engineering and Design, 227, 301–312.
3. Liu, T.J., Bankoff, S.G. (1993) Structure of air–water bubbly flow in a vertical pipe - I. Liquid mean velocity and turbulence measurements. Int. J. Heat Transf. 36, 1049–1060.

4. Ohba, K., Yuhara, T. (1982) Study on vertical bubbly flow using laser doppler measurements. Trans. Jpn. Soc. Mech. Eng. 48 (425), 78–85.
5. Murai1, Y., Oishi1, Y., Takeda1 Y. and Yamamoto, F. (2006) Turbulent shear stress profiles in a bubbly channel flow assessed by particle tracking velocimetry. Experiments in Fluids, 41(2), 343-352.
6. Deen, N.G., Solberg, T. and Hjertager, B.H. (2001) Large Eddy Simulation of the Gas-Liquid Flow in a Square Cross-sectioned Bubble Column. 5th Int. Conf. on Gas-Liquid and Gas-Liquid-Solid Reactor Engineering, Melbourne, Australia, 23-27 Sept. 2001.
7. Delnoij, E., Lammers, F.A., Kuipers, J.A.M. and Van Swaaij, W.P.M. (1997). Dynamic simulation of dispersed gas-liquid two-phase flow using a discrete bubble model. Chemical Engineering Science, 52, 1429-1458.
8. Sokolichin, A., Eigenberger, G., Lapin, A. and Lubbert, A. (1997) Dynamic numerical simulations of gas-liquid two-phase flows, Euler/Euler versus Euler/Lagrange. Chemical Engineering Science, **52**, 611-626.
9. Ishii, M. & Zuber, N. (1979). Drag coefficient and relative velocity in bubbly, droplet or particulate flows. AIChE Journal, 25(5), 843-855.
10. Lopez de Bertodano, M., (1991) Turbulent Bubbly Flow in a Triangular Duct, Ph. D. Thesis, Rensselaer Polytechnic Institute, Troy New York.
11. Lopez de Bertodano, M., (1998) Two Fluid Model for Two-Phase Turbulent Jet, Nucl. Eng. Des. 179, 65-74.

.

7. NOMENCLATURE

Symbol	Meaning	Unit
C_D	drag coefficient	
C_L	lift model constant	
C_{TD}	turbulent dispersion coefficient	
C_1, C_2	model constants for wall lubrication force	
C_{VM}	model constant for virtual mass	
d_b	bubble diameter	(m)
Eo	dimensionless Eotvos number	
$\mathbf{F_D}$	drag force	(N)
$\mathbf{F_L}$	lift force	(N)
$\mathbf{F_{TD}}$	turbulent dispersion force	(N)
$\mathbf{F_{WL}}$	wall lubrication force	(N)
$\mathbf{F_{VIM}}$	virtual mass force	(N)
$\mathbf{F_{kM}}$	summation of all interfacial force	(N)
$\mathbf{g}$	gravity	(m/sec^2)
$\mathbf{n_w}$	unit normal pointing away from the wall	
p	pressure	(pa)
u_r	relative velocity between phases	(m/sec)
$\mathbf{u_k}$	velocity of each phase	(m/sec)
y_w	distance to the nearest wall	(m)
z	axial distance	(m)
ρ_k	density of each phase	(kg/m^3)
α_k	volume fraction of each phase	
μ	dynamic viscosity	(Pa.s)